JVST A
Journal of Vacuum Science & Technology A

Effect of nitrogen contents on the temperature dependence of photoluminescence in In Ga As N Ga As single quantum wells

Fang-I Lai, S. Y. Kuo, J. S. Wang, H. C. Kuo, S. C. Wang, H. S. Wang, C. T. Liang, and Y. F. Chen

Citation: Journal of Vacuum Science & Technology A **24**, 1223 (2006); doi: 10.1116/1.2208996
View online: http://dx.doi.org/10.1116/1.2208996
View Table of Contents: http://scitation.aip.org/content/avs/journal/jvsta/24/4?ver=pdfcov
Published by the AVS: Science & Technology of Materials, Interfaces, and Processing

---

Effect of nitrogen contents on the temperature dependence of photoluminescence in InGaAsN/GaAs single quantum wells

Fang-I Lai[a)]
Department of Electronic Engineering, Ching Yun University, 229, Chien-Hsin Road, Jung-Li, 320 Taiwan, Republic of China

S. Y. Kuo
Instrument Technology Research Center, Hsinchu, 300, Taiwan, Republic of China

J. S. Wang
Department of Physics, Chung Yuan Christian University, Chung Li, 320, Taiwan, Republic of China

H. C. Kuo and S. C. Wang
Department of Photonics and Institute of Electro-Optical Engineering, National Chiao-Tung University, Hsinchu, 300, Taiwan, Republic of China

H. S. Wang, C. T. Liang, and Y. F. Chen
Department of Physics, National Taiwan University, Taipei, 106, Taiwan, Republic of China

(Received 4 May 2005; accepted 1 May 2006; published 21 June 2006)

A series of InGaAsN/GaAs single-quantum wells (SQWs) with N contents varied from 0% to 5.3% were grown by molecular-beam epitaxy using a solid As and a nitrogen plasma sources. The impact of nitrogen concentration on the optical properties, as determined by the temperature dependence of photoluminescence (PL), of a 6 nm SQW was investigated. In the low-temperature region, a pronounced temperature-dependent S-shaped peak position was observed in PL spectra while increasing the nitrogen concentration. Quenching behavior reveals that the defect-related nonradiative processes might be enhanced in the highly nitrogen incorporated samples and thus influence the recombination dynamics. In addition, the evolution of the peak position of the InGaAsN/GaAs samples was in agreement with the empirical Varshni model in the high-temperature region. A significant reduction in the temperature dependence of the emission peak position is analyzed as well, and further confirms the prediction of proposed band anticrossing model of the electronic structure of III-N-V alloys. © *2006 American Vacuum Society.*
[DOI: 10.1116/1.2208996]

I. INTRODUCTION

Heterostructures based on quaternary InGaAsN have recently become a subject of extensive experimental and theoretical studies due to unusual physical properties and a great number of optoelectronic and photonic applications.[1–15] Especially, the possibility of achieving 1.55 μm luminescence emission is of great interest for laser diode applications in optical communications.[16] Despite a strong progress in the development of devices,[17–19] many fundamental parameters and processes still remain unknown or not fully explained. Incorporating nitrogen into GaAs or InGaAs changes the band structure of the host crystal dramatically, which is related to the strong band gap bowing leading to a redshift of the emission wavelength with increasing N concentration.[16,20] A transition from nitrogen acting as an isoelectronic impurity to N-induced band formation has been found in this material system.[21] Much theoretical work has been carried out recently and is still in progress to understand the behavior of nitrogen in InGaAsN.

Compared to InP-based devices, which can easily operate within the desired wavelength window, the quaternary alloy InGaAsN offers several advantages over conventional narrow-gap materials.[22–24] InGaAsN quantum wells (QWs) can be grown pseudomorphically on GaAs, giving strong carrier confinement (hence thermal stability), compatibility with GaAs technology [including AlGaAs/AlAs distributed Bragg reflectors (DBRs)], and extensive control of band gap energy, strain, and band alignment. Even though lasing emission at 1.55 μm has been reported,[17] there seems to be an important fundamental barrier to exceed 1.3 μm emission and reach longer wavelengths due to difficulty in the growth of high-quality InGaAsN/GaAs QW structures with high composition of In or N. Alloying N into InGaAs QWs has proved a challenge due to a low efficiency of N incorporation combined with a large alloy miscibility gap in the phase diagram, and hence InGaAsN tends to phase separate, resulting in the formation of inhomogeneous material with inclusions of diverse phases.[25,26] Xin *et al.* also reported that increasing In concentration in InGaAsN results in a rougher interface.[27] Moreover, larger N and In concentrations cause strong quenching of luminescence, a broadening of luminescence linewidth of the alloys, increase of the nonradiative (monomolecular and Auger) recombination, and thus lower material gain and higher transparency carrier density.[28,29] Accordingly, to achieve a larger incorporation of N or In into

---

[a)] Author to whom correspondence should be addressed; electronic mail: fangi.eo88g@nctu.edu.tw the InGaAsN quantum well requires a more detailed knowledge of the role of the growth conditions on defect formation, and how it impacts the optical properties for both scientific and technological points of view.

In this work, we investigate the optical properties of InGaAsN/GaAs single quantum wells (SQWs) grown by molecular-beam epitaxy (MBE) with various nitrogen contents from 0% to 5.3% at 34% indium and 66% Ga concentrations. The optical properties of the InGaAsN alloys are investigated by the temperature dependence of photoluminescence (PL). SQWs emitting in the wavelength range of 1.05–1.5 μm have been characterized in order to investigate the effects of N incorporation on the mechanisms of recombination process.

II. EXPERIMENTAL PROCEDURE

InGaAsN/GaAs SQWs were grown by MBE on semi-insulating (001)-oriented GaAs substrates. The GaInAsN SQWs were grown using solid sources for group-III and arsenic (As) elements, and an EPI-Unibulb radio-frequency plasma source for supplying active nitrogen species from ultrahigh-purity N_2 gas. The N composition was controlled by monitoring the intensity of the N plasma emission and calibrated from x-ray diffraction (XRD) analysis. High resolution XRD patterns using a Bede four-crystal diffractometer were performed to characterize the structural properties. In addition, the molar fractions of indium and nitrogen were determined from the fitting results of XRD spectra using dynamic simulation software (RADS). During the growth of SQWs, reflection high-energy electron diffraction (RHEED) patterns remain streaky in all samples. This indicates that the three-dimensional growth mode was suppressed under suitable growth conditions even with high nitrogen compositions. To remove the defects caused by low-temperature growth, all samples were *in situ* annealed at 700 °C for 10 min after the GaAs cap layer was grown. A series of samples have been grown with varying nitrogen content while keeping the 34% indium and 66% Ga concentrations. The N compositions in the structures were 0%, 2.2%, 4.1%, and 5.3% for samples A, B, C, and D, respectively.

PL measurement was carried out by the 514.5 nm line of an argon ion laser, and the emission from the samples was dispersed by a monochromator and detected using a thermoelectrically cooled InGaAs detector. The samples were mounted on a cold finger in a helium closed cycle refrigerator coupled with a programmable temperature controller which allows measurements in the 20–300 K temperature range.

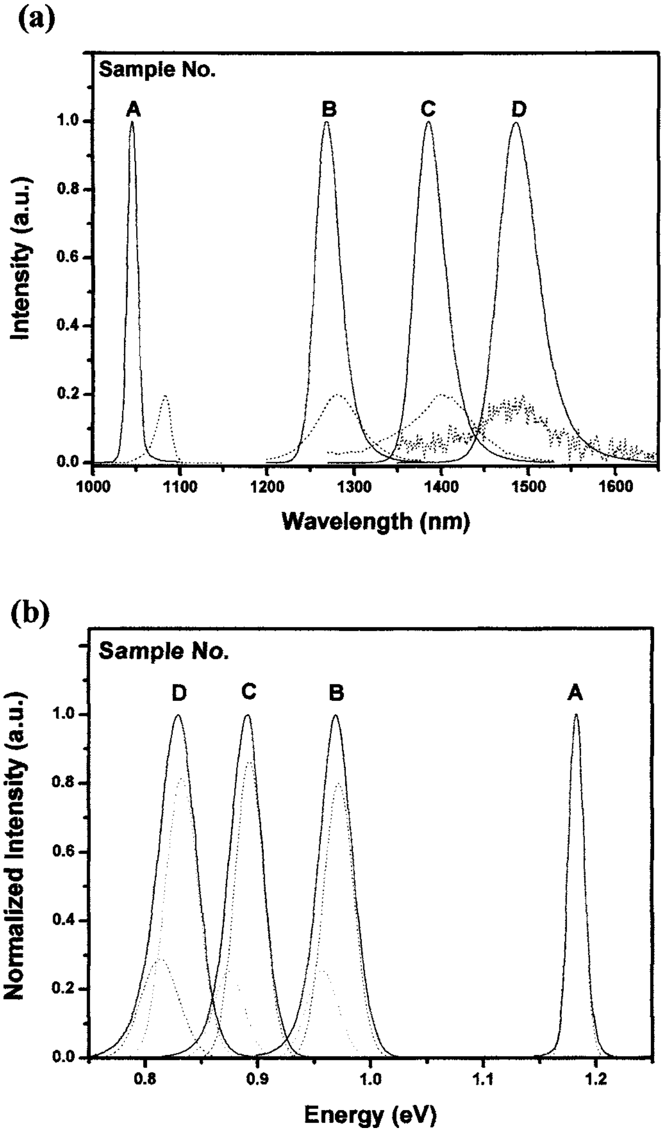

FIG. 1. (a) The 20 K (solid lines) and 190 K (dotted lines) photoluminescence spectra of InGaAsN SQW with different N concentrations. Intensities of the low-temperature spectra were normalized, and appropriate magnification was made on the high-temperature PL spectra to clarify the differences. (b) The fitting results of four InGaAsN samples. Asymmetric line shapes are clearly shown in the nitrogen-incorporation samples.

III. RESULTS AND DISCUSSION

Figure 1(a) shows the low temperature of 20 K (solid lines) and high temperature of 190 K (dotted lines) PL spectra of InGaAsN SQWs with N contents of 0%, 2.2%, 4.1%, and 5.3%, respectively. From the low-temperature PL spectra displayed in Fig. 1(a), it is clearly to see that the PL peaks of the four samples exhibit dissimilar line shape. For sample A without nitrogen incorporation, the emission can be characterized by symmetric, Gaussian-like feature. However, emission from dilute nitride samples shows obvious asymmetric line shape with a sharp high-energy cutoff and an exponential low-energy tail, and should be decomposed into a sum of Gaussian curves.[30–33] A quantitative fit to the PL spectra, assuming a Gaussian distribution of the state density, has been utilized to accurately evaluate the energy peak positions. Fitting results of PL spectra at 50 K are shown in Fig. 1(b) for the InGaAsN SQWs with varied N contents. The conspicuous asymmetric line shape with a low-energy exponential tail for InGaAsN with nitrogen incorporation has been observed in earlier literature as well. The exponential low-energy tail is usually considered to be due to localized states from defects and composition fluctuation.[30] This can be described within the framework of Anderson localization,

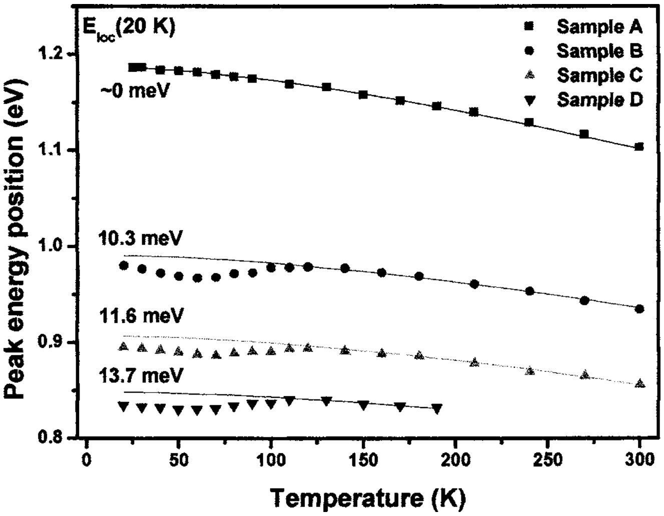

FIG. 2. Temperature dependence of the PL peak energy for the different InGaAsN SQWs. The solid lines represent the results of Varshni fitting and the localization energies $E_{loc}(20\ K)$ are indicated.

where the conduction band edges are smeared so that a tail in the density of states extends into the forbidden gap.[34] At low temperature, photogenerated carriers may be trapped by localized states at the band tail, and the photoluminescence is often originated either from the recombination of spatially separated localized electrons and holes or by electron-hole pairs trapped by potential fluctuations within the same spatial region. Also, a correlation between PL linewidth and nitrogen concentration was exhibited, where the PL linewidth broadens with an increase of N incorporation. This broadening phenomenon indicates that an increasing degree of compositional and structural disorders with increasing nitrogen concentration deteriorates the crystal quality in the quantum wells, which has been extensively reported. Indeed, the highly nitrogen incorporated (5%), sample D, leads to the high-temperature (~190 K) emission at 1.5 μm, close to the frequently targeted 1.55 μm wavelength.

TABLE I. Characteristics of the samples: the molar fraction of nitrogen were determined from the fitting results of XRD spectra, $E_{loc}(20\ K)$ represents the localization energy at 20 K, and E_0, α, and β are the Varshni parameters.

Sample	Nitrogen composition (%)	E_{loc}(20 K) (meV)	E_0 (eV)	α (10^{-4} meV/K)	β (K)
A	0	~0	1.1872	5.8	310
B	2.2	10.3	0.9907	5.35	575
C	4.4	11.6	0.907	5.1	585
D	5.3	13.7	0.8485	4	650

It is expected that the localization centers and their energy distribution in the band gap will be highly dependent on the nitrogen concentration in InGaAsN SQW. We analyze the temperature dependence emission energies to estimate this localization potential. The temperature dependence of the peak energy is depicted in Fig. 2 for the four samples (samples A–D). For sample A, the peak energy redshifts with increasing temperature, which is in good agreement with regular thermalization of carriers. In contrast, other samples with nitrogen incorporation exhibit an anomalous temperature behavior, called S shape. The solid lines represent the fitting results in the high-temperature range using empirical Varshni model,[35]

$$E(T) = E(0) - \frac{\alpha T^2}{T + \beta}, \tag{1}$$

where the $E(0)$, α, and β are the Varshni parameters and T is the measured temperature. All fitting parameters are given in Table I. According to Table I, we find that the thermal stability of the PL peak energy increases (value of α decreases and β increases) with increasing N content, which is consistent with earlier reports. To quantify the S-shape behavior, we measure the mismatch between experimental data and fitted Varshni curves. The carrier localization energy $E_{loc}(T)$ at any temperature is given by the difference $E_{loc}(T) = E(T) - E_{PL}(T)$, where $E_{PL}(T)$ is the temperature-dependent PL peak energy. The results of the Varshni fit and the localization energies at 20 K for all samples are shown in Fig. 2 as well. The S-shape behavior is consistent with that previously attributed to radiative emission of localized carriers found in states below the conduction band edges.[36,37] Between the lowest temperature and the redshift minima, a redshift appears because of the photogenerated carriers gain sufficient thermal energy to thermalize into the lowest available energy state where the recombination takes place. Consequently, the emission of the high energy states is suppressed and a redshift occurs within the range. As the temperature increases further, a blueshift of peak energy occurs. This blueshift could be owing to the thermal equilibrium distribution of the localized carriers increasing and getting close to the delocalized higher energy states. At even higher temperature, the temperature-dependence peak energy is mainly dominated by the behavior of the band-to-band transition and the peak energy will decrease as thermal shrinkage of the gap energy following the normal band gap temperature dependence.

As previously discussed, the effects of localization dominate the low-temperature peak behavior. However, at higher temperatures (above 150 K) the peaks begin to decrease linearly as expected from the Varshni equation.[35] The linear region slope is found to be much smaller for dilute nitride emission than for similar N-free samples (sample A). This behavior can be explained using the band anticrossing (BAC) approach.[1,38] The BAC model of the III-V-N alloys assumes that N atoms substituted in the group-V lattice sites are distributed randomly in the crystal lattice and are coupled weakly to the extended states of the host semiconductor. By solving the eigenvalue problem, the subband energies are given by[38]

$$E_{\pm} = \frac{E_N + E_M \pm [(E_N - E_M)^2 + 4V_{NM}^2]^{1/2}}{2}, \tag{2}$$

where E_N is the energy level of the N localized level and E_M is that of the extended state in the conduction band. V_{NM} is the matrix element describing the coupling between the N

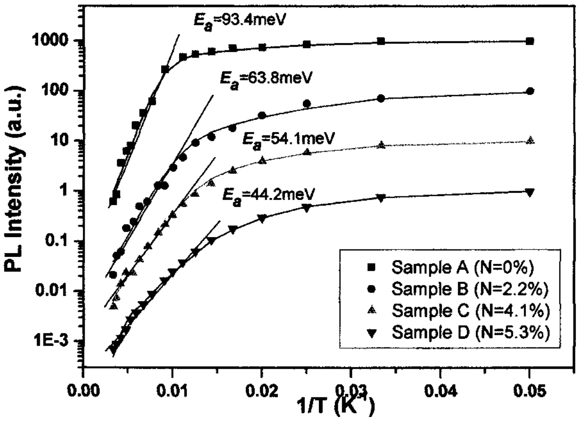

FIG. 3. Plots of normalized integrated PL intensity of the InGaAsN SQWs as function of temperature. The activation energies derived from the slopes of the high temperature region are indicated as solid lines.

localized states and the extended conduction-band state and is given by $C_{NM}x^{1/2}$ under the assumptions of low-N concentrations and random distribution in the group-V sublattice sites. C_{NM} is a constant and x is the N composition in the III-V-N alloys. It is worth noting that a reduction of the linear slope with increasing nitrogen contents indicates that the temperature variation of the emission peak position will be alleviated in the high nitrogen-incorporated samples. An important feature of the BAC model is that the shift of the lower subband E_- depends on the energy difference between E_N and E_M. It indicates that the level repulsion, and thus the reduction of the temperature dependence of the band gap, should be expected to be less pronounced in a semiconductor matrix with E_M located at lower energy. Moreover, Skierbiszewski *et al.*[38] have shown that the hydrostatic pressure dependence of the E_N localized state was about one order of magnitude weaker than that of the InGaAs conduction-band edge, attributed to the localized nature of the N energy level. Based on the information on stability of the N localized state, we can assume the constant energy level E_N in the InGaAsN alloys. Hence, the interaction between the localized E_N level and extended E_M band increases with nitrogen incorporation and the E_- band becomes less like E_M and increasingly like the temperature-insensitive localized state.[39]

In addition, the temperature dependence of integrated intensity of PL was investigated. The curves of normalized integrated PL intensity versus inverse temperature for all samples are plotted in Fig. 3. With an increase in temperature, the overall integrated emission intensity of the PL spectra gradually decreases, indicating the presence of nonradiative recombination centers. The quenching behavior should correspond to the thermally activated nonradiative recombination mechanism, where the slopes give the activation energy. For proper fitting, two thermally activated energies characterized by E_a and E_b were assumed using the following formula:[40]

$$I(T) = \frac{1}{1 + A\exp(-E_a/kT) + B\exp(-E_b/kT)}, \tag{3}$$

where A and B are fitting constants and k is the Boltzmann constant. It is found that the values of E_b for all samples, determined by curve fitting, are in the range of 8–13 meV. Also, the E_b value increases with increasing N concentration and closely correlate with measured E_{loc} values. Hence, the small activation energy of E_b is attributed to trapped excitons or carriers thermalizing from localized regions resulting from potential fluctuation in the SQWs. Besides, the activation energies E_a, derived from the slopes of the straight-line portion (150–300 K) of the curves, are 93.4, 63.8, 54.1, and 44.2 meV for nitrogen compositions of 0%, 2.2%, 4.1%, and 5.3%, respectively. The E_a values decrease with increase of nitrogen incorporation from N contents of 0%–5.3%, which is in agreement with other published works on the trend of the activation energy with increasing N content.[41] This discrepancy might be attributed to different samples and excitation conditions since the recombination dynamics should be dependent on the distribution of localized states. Furthermore, the decrease of E_a can be explained by a higher defect concentration owing to more nitrogen incorporation thus leading to a stronger influence of the defect-related nonradiative processes.

IV. CONCLUSION

In summary, the optical properties of InGaAsN/GaAs SQWs grown by solid-source MBE with various nitrogen contents were investigated by temperature-dependent PL. A pronounced temperature-dependent S shape, attributed to carrier localization effect in the nitrogen-incorporated samples, was exhibited with increasing nitrogen concentration. Also, the emission peak position of N-contained samples has a reduced temperature dependence compared to the N-free InGaAs sample at higher temperatures (above 150 K). This observation could be interpreted using proposed BAC model by assuming a negligible variation in the localized N state with temperature. Furthermore, the activation energy E_a of InGaAsN SQWs is observed to decrease with nitrogen incorporation, contrary to the expectation of band gap reduction, suggesting the existence of defect-related nonradiative processes due to nitrogen incorporation as well. The low-temperature PL exhibits a 1.5 μm emission wavelength with the 5.3% nitrogen concentration and indicates the potential applications for long-wavelength optoelectronic devices.

ACKNOWLEDGMENTS

This work was supported in part by National Science Council of Republic of China (ROC) in Taiwan under Contract No. NSC94-2215-E-009-020 and by the MediaTek Fellowship. The authors would like to thank the Opto-Electronics & Systems Laboratories of the Industrial Technology Research Institute (ITRI) for providing experimental support.

[1] W. Shan, W. Walukiewicz, J. W. Ager III, E. E. Haller, J. F. Geisz, D. J. Friedman, J. M. Olson, and S. R. Krutz, Phys. Rev. Lett. **82**, 1221 (1999).

[2] K. Kim and A. Zunger, Phys. Rev. Lett. **86**, 2609 (2001).

[3] R. J. Potter, N. Balkan, X. Marie, H. Carrere, E. Bedel, and G. Lacoste, Phys. Status Solidi A **187**, 623 (2001).

[4] J.-Y. Duboz, J. A. Gupta, Z. R. Wasilewski, J. Ramsey, R. L. Williams, G. C. Aers, B. J. Riel, and G. I. Sproule, Phys. Rev. B **66**, 085313 (2002).

[5] S. Kurtz *et al.*, Appl. Phys. Lett. **78**, 748 (2000).

[6] V. N. Strocov *et al.*, Phys. Rev. B **69**, 035206 (2004).

[7] T. Kitatani, M. Kondow, and M. Kudo, Jpn. J. Appl. Phys., Part 2 **40**, L750 (2001).

[8] H. D. Sun, M. D. Dawson, M. Othman, J. C. L. Yong, J. M. Rorison, P. Gilet, L. Grenouillet, and A. Million, Appl. Phys. Lett. **82**, 376 (2003).

[9] J. B. Heroux, X. Yang, and W. I. Wang, J. Appl. Phys. **92**, 4361 (2002).

[10] Z. Pan, L. H. Li, Y. W. Lin, B. Q. Sun, D. S. Jiang, and W. K. Ge, Appl. Phys. Lett. **78**, 2217 (2001).

[11] A. Polimeni, M. Capizzi, M. Geddo, M. Fisher, M. Reinhardt, and A. Forchel, Phys. Rev. B **63**, 195320 (2001).

[12] B. Q. Sun, D. S. Jiang, Z. Pan, L. H. Li, and R. H. Wu, Appl. Phys. Lett. **77**, 4148 (2000).

[13] G. Sek, K. Ryczko, J. Misiewicz, M. Fischer, M. Reinhardt, and A. Forchel, Thin Solid Films **380**, 240 (2000).

[14] K. Ryczko, G. Sek, and J. Misiewicz, Solid State Commun. **122**, 323 (2002).

[15] J. Wagner, T. Geppert, K. Kohler, P. Ganser, and N. Herres, J. Appl. Phys. **90**, 5027 (2001).

[16] M. Kondow, K. Uomi, A. Niwa, T. Kitatani, S. Watahiki, and Y. Yazawa, Jpn. J. Appl. Phys., Part 1 **35**, 1273 (1996).

[17] M. O. Fischer, M. Reinhardt, and A. Forchel, IEEE J. Sel. Top. Quantum Electron. **7**, 149 (2001).

[18] M. Fischer, D. Gollub, and A. Forchel, Jpn. J. Appl. Phys., Part 1 **41**, 1162 (2002).

[19] D. Gollub, M. Fischer, and A. Forchel, Electron. Lett. **38**, 1183 (2002).

[20] M. Weyers, M. Sato, and H. Ando, Jpn. J. Appl. Phys., Part 2 **31**, L853 (1992).

[21] P. J. Klar *et al.*, Phys. Status Solidi B **223**, 163 (2001).

[22] M. Kondow, T. Kitatani, S. Nakatsuka, M. Larson, K. Nakahara, Y. Yazawa, and M. Okai, IEEE J. Sel. Top. Quantum Electron. **3**, 19 (1997).

[23] M. Reinhardt, M. Fisher, and A. Forchel, Physica E (Amsterdam) **7**, 919 (2000).

[24] H. D. Sun, M. Hetterich, M. D. Dawson, A. Yu. Egorov, D. Bernklau, and H. Riechert, Appl. Phys. Lett. **92**, 1380 (2002).

[25] J. S. Harris, Jr., Semicond. Sci. Technol. **17**, 880 (2002).

[26] I. A. Buyanova, W. M. Chen, B. Monemar, H. P. Xin, and C. W. Tu, Appl. Phys. Lett. **75**, 3781 (1999).

[27] H. P. Xin, K. L. Kavanagh, Z. Q. Zhu, and C. W. Tu, Appl. Phys. Lett. **74**, 2337 (1999).

[28] Y.-L. Chang *et al.*, Proc.-Electrochem. Soc. **2003-11**, 33 (2003).

[29] J. S. Wang, A. R. Kovsh, R. S. Hsiao, L. P. Chen, J. F. Chen, T. S. Lay, and J. Y. Chi, J. Cryst. Growth **262**, 84 (2004).

[30] I. A. Buyanova, W. M. Chen, G. Pozina, J. P. Bergman, B. Monemar, H. P. Xin, and C. W. Tu, Appl. Phys. Lett. **75**, 501 (1999).

[31] Z. Pan, L. H. Li, W. Zhang, Y. W. Lin, R. H. Wu, and W. Ge, Appl. Phys. Lett. **77**, 1280 (2000).

[32] R. A. Mair, J. Y. Lin, H. X. Jiang, E. D. Jones, A. A. Allerman, and S. R. Kurtz, Appl. Phys. Lett. **76**, 188 (2000).

[33] S. Shirakata, M. Kondow, and T. Kitatani, Appl. Phys. Lett. **80**, 2087 (2002).

[34] P. W. Anderson, Phys. Rev. **109**, 1492 (1958).

[35] Y. P. Varshni, Physica (Utrecht) **34**, 149 (1967).

[36] I. A. Buyanova, W. M. Chen, and C. W. Tu, Semicond. Sci. Technol. **17**, 815 (2002).

[37] M.-A. Pinault and E. Tournié, Appl. Phys. Lett. **78**, 1562 (2001).

[38] C. Skierbiszewski *et al.*, Appl. Phys. Lett. **76**, 2409 (2000).

[39] I. Suemune, K. Uesugi, and W. Walukiewicz, Appl. Phys. Lett. **77**, 3021 (2000).

[40] J. D. Lambkin, L. Considine, S. Walsh, G. M. O'connor, C. J. McDonagh, and T. J. Glynn, Appl. Phys. Lett. **65**, 73 (1994).

[41] S. Shirakata, M. Kondow, and T. Kitatani, Appl. Phys. Lett. **79**, 54 (2001).